Spiral Breakup in Model Equations of Action Potential Propagation in Cardiac Tissue

Alain Karma
Physics Department, Northeastern University, Boston, Massachusetts 02115
(Received 23 March 1993)

Two-variable model equations that capture some essential dynamical features of quantitative electrophysiological models of cardiac tissue are introduced. In one dimension, these equations naturally reproduce an experimentally observed oscillatory pulse instability that causes an alternation in action potential duration. In two dimensions, spontaneous spiral breakup leading to a spatially disorganized electrical wave activity is shown to occur as a direct consequence of this instability.

PACS numbers: 82.40.Fp, 87.90.+y

One possible mechanism which is currently believed to be responsible for the sudden transition from ventricular tachycardia to fibrillation is the spontaneous breakup of a single spiral wave of electrical activity [1] into multiple spirals leading to a turbulent wave behavior. There have been several reports of irregular wave activity in theoretical studies of excitable media [2–4], the most quantitative to date [3,4] being based on electrophysiological models of heart-cell action potential [5,6]. They have provided supportive theoretical evidence that spontaneous spiral breakup may actually occur in cardiac tissue. However, the dynamical origin of this breakup and the condition for its occurrence have remained poorly understood. Perhaps one of the reasons for this is that, due to their complexity, electrophysiological models are not easily tackled analytically and are extremely difficult to simulate in more than one dimension (prohibitively so in three dimensions).

The purpose of this Letter is twofold [7]. The first is to introduce two-variable partial-differential model equations of electrical wave propagation in cardiac tissue. The second is to explain, within the context of these equations, the dynamical mechanism of spiral breakup and pinpoint more precisely the condition for its occurrence. The standard two-variable FitzHugh-Nagumo model with a simple cubic nonlinearity [8], which has been the main focus of recent theoretical investigations [9], is known to support rigidly rotating spiral waves which are unstable over a wide range of parameters. However, in an isotropic continuous excitable media, this instability has always been observed numerically to give rise to a meandering motion of the spiral tip, but not to spontaneous spiral breakup leading to a complex wave behavior. To construct the model equations we have therefore chosen to use as a guide Noble's original adaptation [5] of the classic Hodgkin-Huxley equations [10] to the Purkinje fiber. Although intended to describe this fiber, the Noble model already reproduces some basic properties of the action potential of bulk myocardium tissue [11], and appears to support spiral waves which break up spontaneously [3]. For this reason it provides a natural starting point for identifying the minimum ingredients necessary for this breakup. The four-variable Noble model takes the form

$$C\frac{\partial E}{\partial t}=\nabla^2 E-(E-E_{\mathrm{Na}})[\bar{g}_{\mathrm{Na}}m^3h+\tilde{g}_{\mathrm{Na}}]-(E-E_{\mathrm{K}})[g_{K_1}(E)+g_{K_2}(n)]\,, \tag{1}$$

$$\frac{\partial y}{\partial t}=[y_\infty(E)-y]/\tau_y(E),\quad y=h,m,n\,, \tag{2}$$

where E is measured in mV and C is the membrane capacitance. The variables m and h describe the dynamics of the *fast* sodium ion (Na^+) channel and the variable n the dynamics of a *slow* potassium ion (K^+) channel K_2. The second and third terms on the right-hand side of Eq. (1) represent the membrane currents associated with these channels. The various parameters and functional dependencies of the model are given in Ref. [5]. To change the character of the above equations from spontaneously oscillatory to excitable we have used the procedure of Ref. [3] which consists in slightly lowering the value of $\tilde{g}_{\mathrm{Na}}$ from its standard value 0.14 to 0.132. An *isolated* pulse obtained by numerically solving Eqs. (1) and (2) is displayed in Fig. 1(a). The associated nullcline structure of the Noble model is shown in Fig. 1(b). The latter was constructed by adiabatically eliminating the fast variables h and m of the Na current which vary slowly in time on the 2-3 and 4-1 portions of the cycle. Accordingly, the E-nullcline is defined by $f_E(E,n)=0$, where $f_E(E,n)$ is equal to the right-hand side of Eq. (1) (without the Laplacian term), with $h=h_\infty(E)$ and $m=m_\infty(E)$. The n-nullcline is defined by $f_n(E,n)=0$, where $f_n(E,n)$ is equal to the right-hand side of Eq. (2) with $y=n$. There are three essential properties of the Noble which are absent in the standard FitzHugh-Nagumo model.

(i) Wave-front insensitivity.—The first property is the extremely weak dependence of the wave-front velocity $c_F(n)$ on the slow variable n which controls the action potential duration (APD) (2-3 in Fig. 1). In the FitzHugh-Nagumo model, $c_F(n)$ is known to be a monotonously decreasing function of n which, at leading order in ϵ, vanishes at a stall value $n_S=0$. The corresponding function $c_F(n)$ was calculated by numerically integrating Eqs. (1) and (2) for frozen values of n varying between $n=n_0=0.084$ and $n=1$, and found to only change by a few percent over this interval. This insensitivity is a direct consequence of the wave-front dynamics being con-

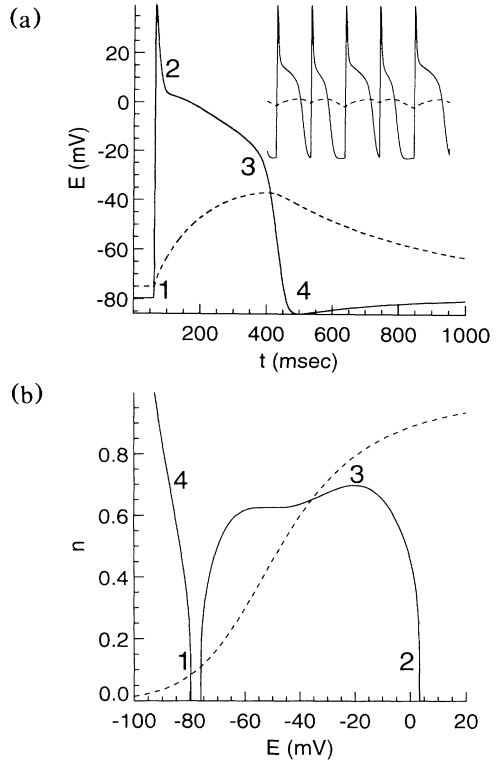

FIG. 1. (a) $E(t)$ (solid line) and $-80+60n(t)$ (dashed line on the same scale) at a fixed position and, upper right, characteristic alternation in APD for a pulse propagating in a ring; (b) E-nullcline (solid line) and n-nullcline (dashed line).

trolled predominantly by the fast variables (m,h) of the Na current.

(ii) Phase-wave back.—The second property relates to the fact that the wave back (3-4 in Fig. 1) is always initiated at the limit point where the rightmost stable branch and unstable middle branch of the E-nullcline meet [point 3 in Fig. 1(b)]. The position of the wave back $X_B(t)$ is therefore defined by the constant *phase condition*, $n(X_B(t),t)=n_B$, where $\partial f_E(E,n_B)/\partial E = f_E(E,n_B)=0$. As a direct consequence, the repolarization period of the wave back ($\tau_B \equiv 3$-4) is much longer than the fast depolarization period of the wave front ($\tau_F \equiv 1$-2).

(iii) Alternans.—The third property is the presence of a known oscillatory pulse instability which occurs on one wavelength of the plane wave train when the train period becomes less than a minimum value $T_{\min}$ ($\simeq$250 msec in the Noble model). This instability causes the duration of the action potential to alternate in time as shown in Fig. 1. These alternans in APD have been observed in periodically driven aggregates of ventricular cells [12] and in rings of cardiac tissue [13], as well as in numerical simulations of the Beeler-Reuter cable equations [14–16]. They have also been modeled previously in terms of maps [12,14,17] and a recently proposed neutral delay-

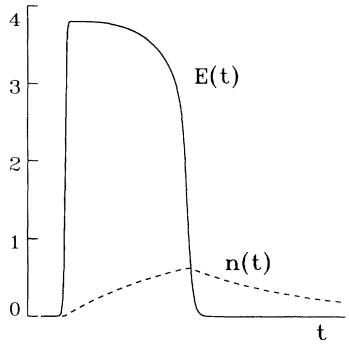

FIG. 2. Characteristic pulse structure generated by the model equations for small ϵ and large M.

differential equation [16].

Two-variable model equations that capture qualitatively all of the above three essential properties take the form

$$\epsilon\frac{\partial E}{\partial t}=\epsilon^2\nabla^2 E-E + \left[A-\left(\frac{n}{n_B}\right)^M\right][1-\tanh(E-3)]\frac{E^2}{2}, \quad (3)$$

$$\frac{\partial n}{\partial t}=f_n(E,n)=\theta(E-1)-n, \quad (4)$$

where $\theta(x)$ is the standard Heaviside step function, ϵ is the usual parameter characterizing the abruptness of excitation, and the constant $A=1.5415$ is chosen such that $\partial f_E(E,n_B)/\partial E = f_E(E,n_B)=0$ [$f_E(E,n)$ now defined by the right-hand side of Eq. (3) without the Laplacian]. These equations have an excitable fixed point $(E_0,n_0)=(0,0)$ and a nullcline structure qualitatively similar to that of Fig. 1(b) over the range $E=(0,4)$. A crucial element is that the wave-front insensitivity is controlled by the parameter M. In the limit $\epsilon \ll 1$ and $M \gg 1$, the front velocity is easily shown to become independent of n [with $dc_F(n)/dn \sim 1/M$] and to approach a step function $c_F(n)=c_0\theta(n_B-n)$. The parameter n_B controls the APD of the isolated pulse (2-3) which takes the simple form $D_0=-\ln(1-n_B)$ in the same limit and, generally, increases with n_B. The phase-wave character of the back (3-4) is implicit in the nullcline structure of the model with the widths of the wave-front and the wave-back scaling, respectively, as ϵ and $(\epsilon/M)^{1/2}$, unlike in the FitzHugh-Nagumo model where both scale as ϵ. The characteristic pulse structure generated by Eqs. (3) and (4) is shown in Fig. 2. Finally, the threshold of the oscillatory pulse instability can be determined exactly in the limit $\epsilon \ll 1$ and $M \gg 1$ using the standard singular perturbation approach used previously in the context of the FitzHugh-Nagumo model [18]. A straightforward calculation [7] yields that the pulse dynamics in that limit is governed by the one-dimensional map $n_F^{j+1}=R(1-n_F^j)$, where n_F^j is the value of the slow variable n on the wave front at the jth turn in a one-dimensional ring of size c_0T,

and $R = n_B e^{-T}/(1-n_B)$. This map has a period doubling subcritical bifurcation at $R=1$ which yields at once the relations $T_{\min}=0$ for $n_B < \frac{1}{2}$ and

$$T_{\min}(n_B) = \ln\left(\frac{n_B}{1-n_B}\right) \text{ for } n_B > \tfrac{1}{2} . \quad (5)$$

These relations define the neutral stability boundary of the oscillatory pulse instability in the (n_B, T) plane at leading order in ϵ and $1/M$. Note that for $n_B < \frac{1}{2}$ the pulse is always stable at this order. Numerical simulation of Eqs. (3) and (4) indicates that finite ϵ and $1/M$ corrections change the nature of the bifurcation from subcritical to supercritical and simultaneously shift the oscillatory dynamics away from exact period doubling. A stable pulse dynamics with quasiperiodically modulated alternans in APD is therefore observed in the present model (Fig. 3) over a range of circulation period $T_{\text{term}} < T < T_{\min}$ (with $T_{\text{term}} \to T_{\min}$ in the small ϵ large M limit). For periods less than the termination period T_{term}, a pulse can no longer propagate. The existence of this period range of "stable alternans" is in agreement with previous studies of electrophysiological models [14,16,17] and our numerical investigation of the Noble model where $T_{\text{term}} \simeq 210$ msec.

The preceding analysis provides the essential basis for our numerical investigation of spiral breakup in two dimensions. Several crucial questions regarding this breakup immediately come to mind: (i) How and when does it occur? (ii) What type of wave behavior does it generate? (iii) What is the role of the boundaries and the system size? (iv) What is the role of meander? We summarize here the answers to these interrelated questions, some definite and others still partial, that we have obtained by extensive numerical simulations of Eqs. (3) and (4) on large square lattices with no flux boundary condition. The answer to the first question is that spiral breakup occurs as a direct consequence of the oscillatory pulse instability [19] when the spiral rotation period T_S, determined numerically by calculating the average cycle length at a fixed position away from the tip, becomes less than some critical value T_{BU} which falls inside the range $T_{\text{term}} < T_{BU} < T_{\min}$. The precise value of T_{BU} within this range was found to depend sensitively on the initial conditions, the lattice size, and the values of the model parameters ϵ, M, and n_B, in a way which we do not presently know how to predict systematically aside from numerical simulation. However, what is definite in the present model is that alternans in APD of sufficiently large amplitude can break up an isolated rotating spiral and that T_{term} and $T_{\min}$ provide useful bounds for T_{BU}. A typical time sequence illustrating the breakup mechanism is shown in Fig. 4. The alternation of APD causes the width of the excited region to vary nonuniformly along the spiral boundary and, thus, breakup to take place where the front is thinnest. In addition, we found that T_S depends weakly on n_B (equivalently on the APD of the isolated pulse) but scales proportionally to $\epsilon^{1/2}$ for small ϵ which explains why spiral breakup always occurred upon decreasing ϵ at fixed $n_B > \frac{1}{2}$, in which case $T_{\min}$ is finite [Eq. (5)], or equivalently by increasing n_B at fixed ϵ. It is interesting to note that this $\epsilon^{1/2}$ scaling of T_S differs from the $\epsilon^{1/3}$ Fife's scaling, which is now well established both

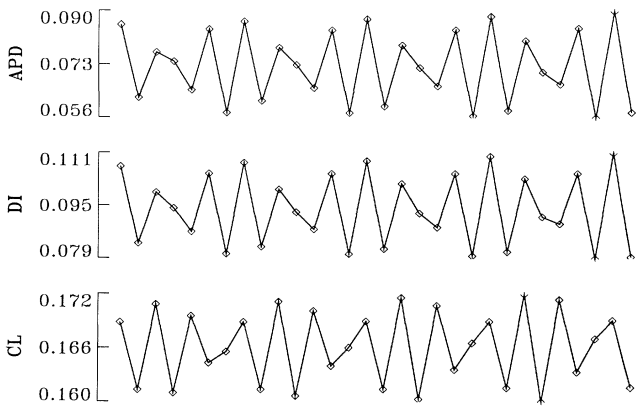

FIG. 3. Oscillatory pulse dynamics observed in simulation of the model equations in a ring of size $L=0.216$ with $\epsilon=0.009$, $M=30$, and $n_B=0.525$. Following the notation of Ref. [13], we have plotted the following as a function of the number of turns in the ring: the APD, defined as the time interval between the passage of the wave front and wave back at a fixed position with $E=2$ as threshold, the diastolic interval (DI), defined as the time interval between the passage of the preceding wave back and the next wave front, and the cycle length (CL), defined as the interval between the passage of two successive wave fronts.

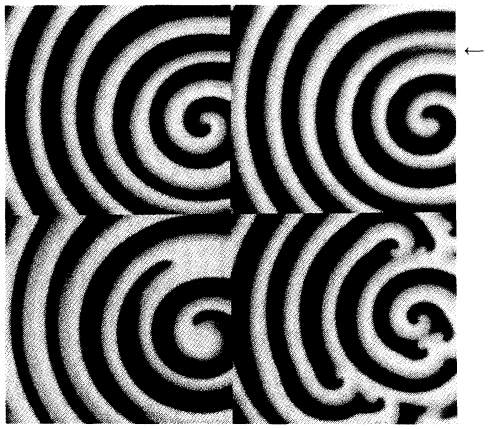

FIG. 4. Time sequence illustrating the dynamical mechanism of spiral breakup in a square lattice of side $L=1.15$ with $n_B=0.507$, $M=30$, and $\epsilon=0.009$: $t=0$ (upper left), $t=0.09$ (upper right), $t=0.135$ (lower left), and $t=1.8$ (lower right); the average rotation period is $T_S \simeq 0.165$. Dark and white regions correspond, respectively, to excited and recovery regions. The location where breakup is initiated at $t=0.09$ is indicated by an arrow.

numerically and analytically for the FitzHugh-Nagumo model [9]. Its existence is almost certainly related to the presence of a phase-wave back, whose width also scales as $\epsilon^{1/2}$, but a quantitative theory of spiral period selection for this new class of model equations remains to be developed to understand this scaling. In regard to question (ii), we observed in all simulations performed until now that breakup of an isolated spiral led to the generation of additional spirals (Fig. 4) which, after a complicated dynamical transient lasting between 10 and 100 basic rotation periods, settled into a "spiral glass" state in which an ensemble of spirals with randomly distributed centers remains essentially frozen in space, aside from a localized meandering motion of the individual tips. It should be emphasized that this type of fibrillatory state is not spatiotemporally chaotic but nonetheless generates complex reentrant pathways of electrical activity which, *in vivo*, could inhibit the heart muscle from pumping coherently and lead to sudden death. In regard to question (iii), we found that spirals were generally attracted to the boundaries and, more importantly, that for a given set of parameters breakup could be suppressed by choosing the system size smaller than some minimum size comparable to a spiral wavelength. This suppression is consistent with the fact that breakup takes place away from the spiral tip and could explain why spontaneous spiral breakup has not been observed in the experiments carried out to date [1] on relatively small pieces of heart tissue. Finally, in regard to question (iv), we observed the usual type of spiral meander observed in the FitzHugh-Nagumo model to be present before, in the single spiral state, and after breakup, in the spiral glass state. This meander may play an auxiliary role in the breakup mechanism which remains to be explored. However, what seems certain at present is that it does not alone induce breakup. This was clearly demonstrated by simulation runs with $n_B < \frac{1}{2}$ where alternans were absent (i.e., $T_{\min}=0$), and breakup was never observed down to very small values of ϵ.

To conclude we note that other important effects (such as spatial inhomogeneities, electromechanical coupling, etc.) not included in the present model may also play an important role in the transition from ventricular tachycardia to fibrillation. However, without these added complications, alternans already suffice to induce a spatially disorganized electrical wave activity and provide a natural mechanism for this transition.

I wish to thank H. Levine and A. Winfree for very fruitful exchanges. This research was supported by the Donors of the Petroleum Research Fund. The hospitality of the ITP at Santa Barbara and support of NSF Grant No. PHY89-04035 are acknowledged.

[1] Spiral waves in isolated 1–2 cm^2 pieces of cardiac tissue have recently been visualized using a voltage sensitive dye by J. M. Davidenko, P. Kent, and J. Jalife, Physica (Amsterdam) **49D**, 182 (1991); J. M. Davidenko, A. V. Pertsov, R. Salomonsz, W. Baxter, and J. Jalife, Nature (London) **355**, 349 (1992). Earlier pioneering experiments using a network of electrodes were performed by M. A. Allessie, F. I. M. Bonke, and F. J. G. Schopmann, Circ. Res. **33**, 54 (1973).

[2] J. M. Smith and R. J. Cohen, Proc. Natl. Acad. Sci. U.S.A. **81**, 233 (1984); M. Gerhardt, H. Schuster, and J.J. Tyson, Science **247**, 1563 (1990); H. Ito and L. Glass, Phys. Rev. Lett. **66**, 671 (1991).

[3] A. V. Holden and A. V. Panfilov, Int. J. Bifurcation Chaos **1**, 219 (1991).

[4] A. T. Winfree, J. Theor. Biol. **138**, 353 (1989); M. Courtemanche and A. T. Winfree, Int. J. Bifurcation Chaos **1**, 431 (1991).

[5] D. Noble, J. Physiol. **160**, 317 (1962).

[6] G. W. Beeler and H. Reuter, J. Physiol. **268**, 177 (1977).

[7] A. Karma (to be published).

[8] R. FitzHugh, Biophys. J. **1**, 445 (1961); J. Nagumo, S. Arimoto, and S. Yoshizawa, Proc. IRE **50**, 2061 (1962).

[9] A. T. Winfree, Chaos **1**, 303 (1991); P. Pelce and J. Sun, Physica (Amsterdam) **48D**, 353 (1991); A. Karma, Phys. Rev. Lett. **68**, 397 (1992); D. A. Kessler, H. Levine, and W. N. Reynolds, Phys. Rev. Lett. **68**, 401 (1992); D. Barkley, Phys. Rev. Lett. **68**, 2090 (1992); J. P. Keener, SIAM J. Appl. Math. **52**, 1370 (1992).

[10] A. L. Hodgkin and A. F. Huxley, J. Physiol. **117**, 500 (1952).

[11] G. R. Ivanitsky, V. I. Krinsky, and E. E. Sel'kov, in *Mathematical Biophysics of the Cell* (Nauka, Moscow, 1978); V. S. Zykov, *Simulation of Wave Processes in Excitable Media* (Manchester Univ. Press, New York, 1987).

[12] M. R. Guevara, G. Ward, A. Shrier, and L. Glass, in *Computers in Cardiology* (IEEE Compuer Society Press, Salt Lake City, 1984), p. 167.

[13] L. H. Frame and M. B. Simson, Circulation **78**, 1277 (1988).

[14] T. Lewis and M. R. Guevara, J. Theor. Biol. **146**, 407 (1990).

[15] W. Quan and Y. Rudy, Circ. Res. **66**, 367 (1990); PACE, Process Control Eng. **14**, 1700 (1991).

[16] M. Courtemanche, L. Glass, and J. P. Keener, Phys. Rev. Lett. **70**, 2182 (1993).

[17] H. Ito and L. Glass, Physica (Amsterdam) **56D**, 84 (1992).

[18] J. P. Keener, SIAM J. Appl. Math. **39**, 528 (1980).

[19] Spiral breakup in oscillatory media described by the complex Ginzburg-Landau equation occurs by an analogous mechanism, the role of the short-wavelength oscillatory instability present here being played by the long-wavelength Benjamin-Feir instability: Y. Kuramoto and S. Koga, Prog. Theor. Phys. **66**, 1081 (1981); P. Coullet, L. Gil, and J. Lega, Phys. Rev. Lett. **62**, 1619 (1989); I. S. Aronson, L. Aronson, L. Kramer, and A. Weber, Phys. Rev. A **46**, R2992 (1992).

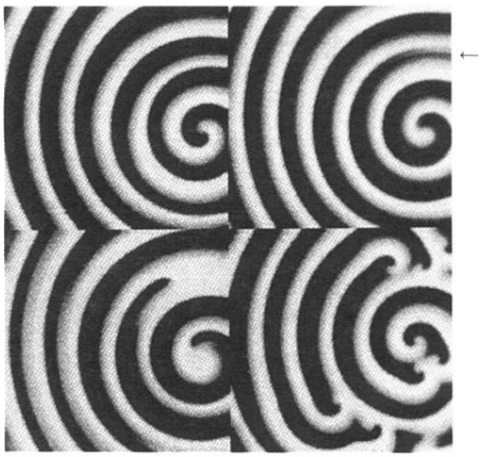

FIG. 4. Time sequence illustrating the dynamical mechanism of spiral breakup in a square lattice of side $L=1.15$ with $n_B=0.507$, $M=30$, and $\epsilon=0.009$: $t=0$ (upper left), $t=0.09$ (upper right), $t=0.135$ (lower left), and $t=1.8$ (lower right); the average rotation period is $T_S\simeq 0.165$. Dark and white regions correspond, respectively, to excited and recovery regions. The location where breakup is initiated at $t=0.09$ is indicated by an arrow.